American Mineralogist, Volume 81, pages 639–650, 1996

A reexamination of absorption and enhancement effects in X-ray fluorescence trace element analysis

Rex A. Couture and Robert F. Dymek

Department of Earth and Planetary Sciences, Washington University, Box 1169, 1 Brookings Drive, St. Louis, Missouri 63130, U.S.A.

Abstract

In this paper, sample mass-absorption corrections for X-ray fluorescence trace element analysis are reexamined and a new approach is presented that is more accurate and more versatile than current methods. A method based on Compton scattering of a tube line is widely used because it is simple and does not require knowledge of the complete sample composition. The equivalent-wavelength method is sometimes used instead, especially if there is a major element absorption edge between the wavelengths of the Compton peak and the characteristic analyte radiation. Both methods suffer from difficulties in correcting for absorption edges and for enhancement by secondary fluorescence. In addition, the necessary assumption that the ratio of mass-absorption coefficients of any two elements is approximately independent of wavelength is surprisingly inaccurate. A series of examples demonstrates that in some cases large analytical errors may result.

Methods based on the new approach completely and automatically correct for absorption edges and secondary fluorescence, without introducing such errors. In contrast to current methods, a complete major element analysis is not necessary. Thus, rapid determination of concentration ratios, such as Cr/Fe and V/Fe in oxide ores, Ba/Fe in Fe-rich hydrothermal deposits, and Sr/Ca in carbonates, is possible.

In an experimental test, accuracy of better than 1% was demonstrated for analysis of V in Fe-rich samples. A proposed coefficient approximation was shown to give accuracy of 2% or better (excluding experimental errors) for Rb, Ni, Ba, and Cr over an extremely wide range of sample compositions.

Introduction

Absorption-enhancement corrections for X-ray fluorescence (XRF) analysis require extensive computation and involve integration of a sample-specific function over wavelength. For trace element analysis, the problem can be simplified in various ways. With the Compton-peak method, Compton scattering of a tube-target line is commonly used to estimate sample mass-absorption coefficients (cf. Hower 1959; Reynolds 1963, 1967). Because the Compton mass-scattering cross section is roughly independent of atomic number, the intensity of Compton scattering is determined mainly by absorption in the sample. The result is that the intensity of a Compton peak is approximately inversely related to the mass-absorption coefficient of the sample. This relationship can be used to correct for absorption without knowledge of the major element composition of the sample or of any binder or diluent that might be added.

For quantitative XRF analysis using the Compton-peak method, the main assumptions are as follows: (1) The sample has no absorption edges between the Compton-peak wavelength and the analyte-peak wavelength; (2) the ratio of mass-absorption coefficients at any two wavelengths is nearly independent of sample composition if there is no intervening absorption edge (Hower 1959); and (3) enhancement effects (secondary and tertiary fluorescence) are unimportant.

These assumptions pose substantial problems for the analyst. The first assumption can be invalidated by major or minor element absorption edges. Analysis for Co, Cr, V, Sc, and Ba in the presence of Fe and Ti are well-known examples. The second assumption is highly inaccurate for some sample matrix elements, especially Fe, Ti, K, Ca, C, and H. Finally, enhancement can be extremely important in some samples, but it is typically ignored because making the correction is numerically difficult.

The equivalent-wavelength method is closely related to the Compton-peak method and is commonly used instead. The equivalent-wavelength method avoids integration by assuming that a single wavelength, called the equivalent wavelength, can approximate the polychromatic incident spectrum, resulting in greatly simplified mass-absorption calculations. The sample mass-absorption coefficients can be calculated from the composition or from the Compton-peak intensity. If an absorption edge is present between the Compton-peak wavelength and the analyte-peak wavelength, sample mass-absorption coefficients must be calculated on both sides of the absorption edge. For this purpose, an absorption-edge

0003–004X/96/0506–0639$05.00

TABLE 1. Symbols used in this paper

Subscript *i* always refers to the analyte element.	
I_{il}	fluorescent intensity for analyte *i*, line *l*
C_i	concentration (mass fraction) of analyte *i*
λ and λ_i	wavelength and the characteristic analyte wavelength, respectively
λ_{jk}	wavelength of line *k* of element *j*
λ_0	shortest wavelength of the incident spectrum
$\lambda_{\text{edge } i}$	absorption-edge wavelength of the analyte
$I_0(\lambda)$	tube intensity at wavelength λ
ψ_1, ψ_2	average angle of incidence and emergence relative to sample surface
$\mu_s(\lambda)$ and $\mu_i(\lambda)$	mass-absorption coefficient of sample and element *i* at wavelength λ
$\mu_s'(\lambda)$	$\mu_s(\lambda)/\sin\psi_1$
$\mu_s''(\lambda_i)$	$\mu_s(\lambda_i)/\sin\psi_2$
μ_s^*	$\mu_s'(\lambda) + \mu_s''(\lambda_i)$
r_i	photoelectric absorption-jump ratio due to the shell in question
ω_i	the fluorescence yield for that shell
p_{il}	the transition probability, i.e., the intensity of the analytical line *l* relative to all lines from the same shell (e.g., $K\alpha$ intensity relative to total *K* line intensity)
Ω	the solid angle of acceptance by the detector
S	the irradiated sample area
f_{il}	$g_{il}\frac{\Omega}{4\pi}\frac{S}{\sin\psi_2}$
g_{il}	$\frac{r_i - 1}{r_i}\omega_i p_{il}$

jump ratio is sometimes calculated from the element intensity of the absorption edge (Walker 1973). Although the Compton-peak and equivalent-wavelength methods may give satisfactory results in many cases, they require assumptions that are not entirely correct, as is shown in the present work, and they have practical limitations as well. In addition, neither method corrects for enhancement.

The theories of the Compton-peak and equivalent-wavelength methods for trace element analysis were developed by Hower (1959), Reynolds (1963, 1967), Walker (1973), Feather and Willis (1976), and many others. Of course, simplifying assumptions that were necessary in the past, because of the difficulty of the calculations, are no longer necessary owing to advances in computer hardware and in fundamental-parameter and influence-coefficient methods. However, the Compton-peak and equivalent-wavelength methods have not benefited from recent advances, and comprehensive treatments of absorption edges and enhancement are still lacking.

In this paper the fundamental assumptions about trace element analysis are reexamined to clarify the limitations of existing methods and to present a new and different approach. The Compton-peak and equivalent-wavelength methods represent approximations of the fundamental equation and may introduce large errors in calculations. Therefore, the accuracy of these approximations is tested against the fundamental equation, and the resulting errors are illustrated with a series of numerical examples.

Finally, a new approach is presented, which appears to be valid for virtually any sample. It combines the attributes and advantages of the Compton-peak method with those of more general methods. A coefficient method based on this approach is evaluated numerically and experimentally and is shown to be highly accurate and more versatile than previous methods.

THEORY: PRIMARY AND SECONDARY FLUORESCENCE INTENSITY

The theory underlying X-ray fluorescence analysis (Sherman 1955; Shiraiwa and Fujino 1966; Tertian and Claisse 1982; Müller 1972; Jenkins et al. 1981) is well established and accepted. The fundamental equation (Eq. 1), and the influence-coefficient methods based on this equation, give corrections that are sufficiently accurate for major element analysis (cf. Pella and Sieber 1982; Rousseau 1984b; Rousseau and Bouchard 1986; Pella et al. 1986; de Boer et al. 1993; Eastell and Willis 1993; Couture et al. 1993). Therefore, the fundamental equation constitutes an accurate theoretical basis for the evaluation of other methods.

The intensity of a given X-ray line from element *i* is the sum of the primary fluorescence (due to tube radiation), the secondary fluorescence (due to other elements in the sample), the tertiary fluorescence (due to secondary fluorescence of other elements), and so forth. The following presentation does not consider tertiary fluorescence because it is usually quite small. Equations for the tertiary fluorescence intensity were derived by Sherman (1955) and Shiraiwa and Fujino (1966), among others, and Sparks (1975) presented a useful simplification for tertiary fluorescence.

The symbols and definitions used in the following equations are presented in Table 1. The fluorescence intensity I_{il} for analyte *i*, line *l*, is given by

$$I_{il} = f_{il}C_i\left(\int_{\lambda_0}^{\lambda_{\text{edge } i}} A\,d\lambda + \sum_j C_j \int_{\lambda_0}^{\lambda_{\text{edge } j}} AE_j\,d\lambda\right) \quad (1)$$

where

$$A = \frac{\mu_i(\lambda)I_0(\lambda)}{\mu_s^*} \quad (2)$$

and

$$E_j = \frac{1}{2}\frac{\mu_j(\lambda)}{\mu_i(\lambda)}\sum_k g_{jk}\mu_i(\lambda_{jk})L_{jk}. \quad (3)$$

$$L_{jk} = \frac{\ln[1 + \mu_s'(\lambda)/\mu_s(\lambda_{jk})]}{\mu_s'(\lambda)} + \frac{\ln[1 + \mu_s''(\lambda_i)/\mu_s(\lambda_{jk})]}{\mu_s''(\lambda_i)} \quad (4)$$

if $\lambda_{jk} \le \lambda_{\text{edge } i}$ and $\lambda_{jk} > \lambda_0$, or 0 otherwise.

Equation 1 is generally considered to be accurate and correct, but it still entails certain assumptions. Most spectrometers use a widely divergent beam, so an average value for ψ_1 (see Table 1) is assumed, although the correct value may not be easy to determine [cf. Müller (1972, p. 84)]. In addition, the effect of scattering on attenuation is generally ignored, so that total mass-absorption coefficients are used in the denominator. The factor $\mu_i(\lambda)$ in the numerator of Equation 2 is an approximation of the

photoelectric mass-absorption coefficient, and the $1/r^2$ dependence of intensity on distance from the target is ignored. These approximations are not usually considered to be important, especially for trace elements (cf. Müller 1972; Jenkins et al. 1981), and it is not the purpose of this paper to examine these assumptions.

Equation 1 appears quite complicated, but the absorption part is rather simple. The numerator of A (Eq. 2) represents absorption of tube radiation by the analyte element as a function of wavelength. The denominator μ_s^* represents absorption by the sample and consists of two terms: $\mu_s'(\lambda)$ represents absorption of tube radiation, and $\mu_s''(\lambda_i)$ represents absorption of analyte radiation. E_j in Equation 1 corresponds to enhancement by secondary fluorescence. The secondary fluorescence intensity is calculated by summing over each line k of each element j that can cause fluorescence. Both A and E_j depend on the sample composition, so direct solution of Equation 1 for composition requires numerical integration over the spectrum for each sample.

Equation 1 is usually solved by direct calculation of the sample mass-absorption coefficient from published tables, using

$$\mu_s(\lambda) = \sum_j C_j \mu_j(\lambda). \quad (5)$$

An alternative method, based on both composition and the intensity of a Compton-peak–scattered tube line, is presented later. For calibration, intensities are calculated from Equation 1, and f_{ij} is calculated by comparison with measured intensities. For analysis, Equation 1 is solved for composition by iteration. It can also be solved by indirect methods: either the Compton-peak method, the equivalent-wavelength method, or a series approximation (influence coefficients). This paper deals with the methods and accuracy of these approximations.

The Compton-peak method

Principles

Mass-absorption coefficients from the Compton-peak intensity. The atomic Compton-scattering cross section is roughly proportional to the number of electrons and, therefore, to the atomic weight. Consequently, the mass-scattering coefficient, which is the scattering cross section per unit mass, is roughly independent of atomic mass over a limited range of atomic number (see Fig. 1). Because the intensity of the Compton-scattered peak from a thick sample is proportional to the mass-scattering coefficient divided by the mass-absorption coefficient (Tertian and Claisse 1982, p. 261), this ratio is a practical measure of the mass-absorption coefficient.

The mass-scattering coefficient is generally expressed as $d\sigma/d\Omega$, which is the differential cross section per unit solid angle. This parameter was calculated for Rh$K\alpha$ radiation, assuming a scattering angle of 100°. The Klein-Nishina formula for free-electron scattering was used, and values for the theoretical incoherent scattering function $S(x, Z)$ were taken from Hubbell et al. (1975). The mass-scattering coefficients for Rh$K\alpha$ radiation are plotted in Figure 1 as a function of μ_s.

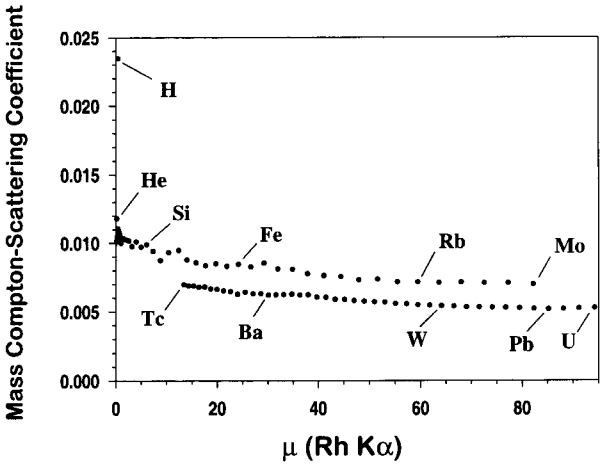

FIGURE 1. Mass Compton-scattering coefficients $d\sigma/d\Omega$ (in squared centimeters per gram) for Rh$K\alpha$ radiation vs. μ (in squared centimeters per gram) at $\lambda_{RhK\alpha}$ for the chemical elements. Over a narrow range of Z, the coefficients are approximately linear with μ.

Over almost any limited range of atomic number the relation between $d\sigma/d\Omega$ and μ_s is approximately linear with μ (cf. Tertian and Claisse 1982, p. 263). If δ_j represents the deviation from a straight line, the coefficient for element j can be represented by

$$\frac{d\sigma_j}{d\Omega} = b + \mu_j d + \delta_j \quad (6)$$

and it is easily shown that

$$I_C = \frac{B + \sum_j C_j \delta_j}{\mu_s(\lambda_t)} + D \quad (7)$$

where I_C is the Compton-peak intensity, λ_t is the wavelength of the tube line, and b, d, B, and D are constants. B, D, and δ_j are easily determined empirically by measuring I_C for known compounds. In most geological applications, δ_j, can be ignored and D is small, giving the familiar reciprocal relation $\mu_s(\lambda_t) = B/I_C$ (cf. Reynolds 1967).

Figure 2 shows a plot of the calculated Compton-peak intensity vs. $1/\mu_s$. For 11 oxides from Na_2O to Fe_2O_3, a linear least-squares fit (with $\delta_j = 0$) gives a relative standard error of the estimate of only ±1.8%. The light elements also showed reasonable conformity using the same fit: H_2O deviates by 14%, and CO_2 deviates by 3.8%; Li_2O and B_2O_3 deviate by only 0.4 and 2.3%, respectively. Overall, such light elements contribute little to the mass-absorption coefficients of most samples. Thus, δ_j can be ignored in ordinary geological applications. However, because of a K absorption edge above Mo, shown in Figure 1, this is not true for samples that contain both light and heavy major elements. Formerly, such samples could not

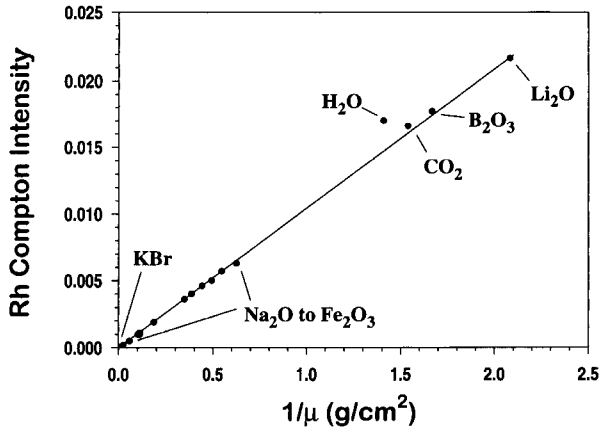

FIGURE 2. Calculated Rh$K\alpha$ Compton-peak intensity vs. $1/\mu$ for 15 oxides from H_2O to Fe_2O_3, plus KBr. Data from Hubbell et al. (1975) and Thinh and Leroux (1979).

be analyzed at all by the Compton-peak method. Fortunately, there are few such geological samples.

As a practical matter, it is difficult to measure the intensity of a Compton-scattered Rh tube line because the peak is superimposed on a strong, irregular background that consists of Compton- and Rayleigh-scattered continuum radiation. For an Mo tube the Raleigh and Compton peaks may be unresolved (Reynolds 1967). In addition, there may be a constant, scattered contribution from sample masks or other spectrometer parts. Nevertheless, Equation 7 appears to be an accurate empirical relation (Couture, unpublished data; Tertian and Claisse 1982, p. 264). It is a common practice to plot $1/I_C$ vs. μ_s, but this generally gives a curve (Reynolds 1967; Harvey and Atkin 1982), whereas Equation 7 gives a straight line.

Hower's approximation and Compton scattering. Hower (1959) observed that the ratio of mass-absorption coefficients of any two elements i and j is approximately independent of wavelength, so that

$$\frac{\mu_i(\lambda_1)}{\mu_j(\lambda_1)} \approx \frac{\mu_i(\lambda_2)}{\mu_j(\lambda_2)} \tag{8}$$

and

$$\frac{\mu_i(\lambda)}{\mu_i(\lambda_t)} \approx \frac{\mu_j(\lambda)}{\mu_j(\lambda_t)} \approx K(\lambda) \tag{9}$$

as long as λ_1 and λ_2 do not span an absorption edge of elements i or j. This is also true for mixtures and compounds, so the wavelength dependence of the mass-absorption coefficient of any sample can be expressed approximately as a single function $K(\lambda)$. In practice, representative values of $K(\lambda)$ can be calculated from Si or SiO_2.

From Equations 7 and 9, the mass-absorption coefficient at any wavelength can be determined from the Compton-peak intensity (assuming $\delta_j = 0$ for brevity):

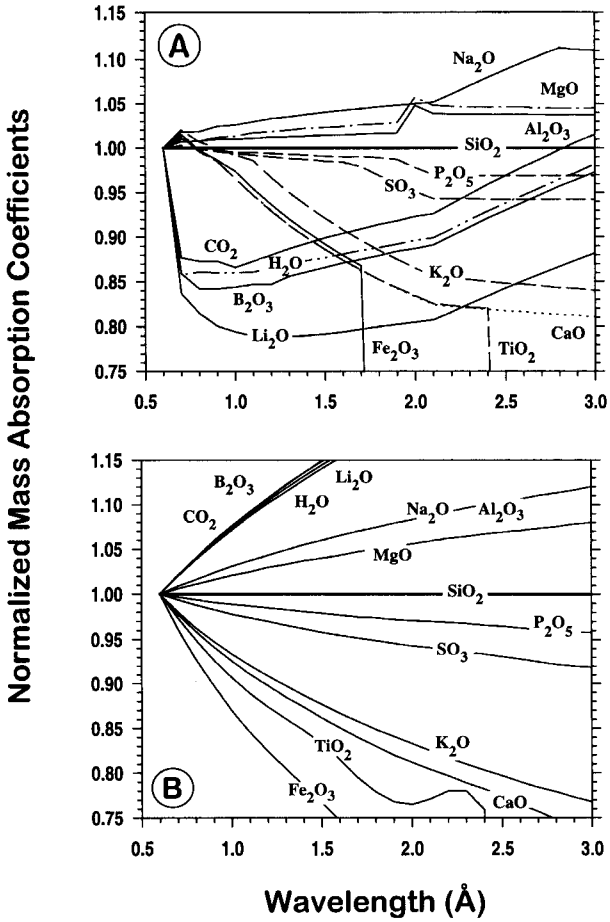

FIGURE 3. (A) Mass-absorption coefficients normalized to SiO_2 and to $\lambda_{RhK\alpha}$ vs. λ. If Hower's approximation (Eq. 9) is correct, the normalized coefficient must be 1 at all wavelengths (see Eq. 14). (B) Photoelectric mass-absorption coefficients normalized to SiO_2 and to $\lambda_{RhK\alpha}$ vs. λ. Data from program XCOM (Berger and Hubbell 1987).

$$\mu_s(\lambda) \approx K(\lambda)\mu_s(\lambda_t) \approx \frac{BK(\lambda)}{I_C - D}. \tag{10}$$

If the sample has no significant (i.e., major element) absorption edge between λ_0 and $\lambda_{edge\ i}$, Equation 10 can be substituted into Equation 1, giving

$$I_{il} \approx C_i(I_C - D)\left[\frac{f_{il}}{B}\int_{\lambda_0}^{\lambda_{edge\ i}} \frac{\mu_i(\lambda)I(\lambda)\,d\lambda}{K'(\lambda) + K''(\lambda_i)}\right] \tag{11}$$

where

$$K'(\lambda) = K(\lambda)/\sin\psi_1 \tag{12}$$

and

$$K''(\lambda) = K(\lambda)/\sin\psi_2. \tag{13}$$

Because there is no intervening absorption edge, there is no secondary fluorescence.

The expression in brackets in Equation 11 is a constant

TABLE 2. Errors (% relative) in the Compton method

Rock*	Total trace elements**	Multiple edges			Hower's approximation			Combined		
		Sr$K\alpha$	Ni$K\alpha$	Cr$K\alpha$	Sr$K\alpha$	Ni$K\alpha$	Cr$K\alpha$	Sr$K\alpha$	Ni$K\alpha$	Cr$K\alpha$
SiO_2	0				0.0	0.0	0.0	0.0	0.0	0.0
Al_2O_3	0				−0.3	−1.0	−2.9	−0.3	−1.0	−2.9
$CaCO_3$	0				1.6	13.8	19.9	1.6	13.8	19.9
50% SiO_2 + 50% Fe_2O_3	0				1.0	11.7		1.0	11.7	
Fe_2O_3	0				1.2	13.4		1.2	13.4	
Feldspar JF-2	0.12	0.9	1.4	1.5	0.0	3.4	5.4	0.9	4.8	7.0
Basalt BCR-1	0.26	0.6	0.9		0.7	8.5		1.3	9.5	
Granite G-2	0.44	2.4	3.4		0.2	3.8		2.6	7.3	
Syenite STM-1	0.5	4.1	5.5		0.3	4.7		4.4	10.5	
Granite MA-N	0.61	6.2	8.8		−0.0	1.5		6.2	10.4	
Shonkinite	0.75	2.2	2.9		1.1	11.9		3.3	15.1	
SiO_2 + 1% SrO	1.0	17.1	23.8	24.3				17.1	23.8	24.3
Ljuvarovite NIM-L	2.35	17.7	23.2		0.6	7.4		18.4	32.4	

Note: Errors due to (1) uncorrected absorption edges (see text), (2) Hower's approximation (Eq. 9), (3) both errors combined. Same tube conditions as in Figure 4.

* Compositions from Govindaraju (1989); Shonkinite is 33.7% SiO_2, 7.3% TiO_2, 2.5% Al_2O_3, 34.8% Fe_2O_3, 4.7% MgO, 12.1% CaO, 0.7% Na_2O, 0.5% K_2O, and 2.5% P_2O_5.

** Total Cr, Co, V, Cu, Zn, Ga, Rb, Sr, Y, Zr, Ba, and Pb (wt%) as oxides.

that can be determined by calibration or by calculation. Equation 11 represents the familiar relation between trace element concentration, intensity, and the Compton-peak intensity. Note that it is not valid if there is any intervening major element absorption edge, including that of the analyte, between λ_0 and λ_i. Therefore, it is not valid for analysis of major elements.

Test of Hower's approximation. Unfortunately, Hower's approximation (Eq. 9) is not at all accurate. Equation 9 can be tested by rewriting it as

$$\frac{\left[\frac{\mu_i(\lambda)}{\mu_i(\lambda_i)}\right]}{\left[\frac{\mu_j(\lambda)}{\mu_j(\lambda_i)}\right]} \approx 1. \quad (14)$$

A plot of this ratio against λ, shown in Figure 3A, reveals deviations of up to 23% over the important wavelength range of 0.6–3 Å. Within a narrow range of atomic number (oxides from Na_2O to SO_3) the approximation is reasonably accurate, generally within 6%, but the light oxides (Li_2O through CO_2) and heavier oxides (K_2O through Fe_2O_3) have anomalously low mass-absorption coefficients at intermediate wavelengths. The patterns are generally similar whether the mass-absorption coefficients of Thinh and Leroux (1979), Heinrich (1986), or the program XCOM (Berger and Hubbell 1987) are used, although there is disagreement about the lightest elements. If only the photoelectric mass-absorption coefficients are plotted, as in Figure 3B, the situation is similar except for the lightest elements, which have anomalously high coefficients at intermediate wavelengths.

Accuracy of the Compton-peak method

In addition to errors resulting from Hower's approximation (Eq. 9), the Compton-peak method is subject to errors resulting from multiple uncompensated absorption edges in those rocks that have unexpectedly high concentrations of trace elements. These errors were evaluated for a variety of rock types, by comparing the results from Equations 1 and 11, with the use of the method presented in the Appendix.

The errors estimated for several rocks are shown in Table 2. For this calculation SiO_2 was used as a reference, i.e., it was assumed that SiO_2 is representative of all components of the rock, and thus that the ratio of the mass-absorption coefficient of the rock to that of SiO_2 is independent of wavelength. Sr, Ni, and Cr were selected to represent the range of trace element wavelengths customarily analyzed with an Rh tube. For Fe-containing samples, values are not shown for Cr because the method is not valid.

For Sr$K\alpha$ the total range of errors due to Hower's approximation is small, only −0.3 to 1.6%, because the wavelength (0.877 Å) is close to that of Rh (0.615 Å). The errors are larger for longer wavelengths and are serious for transition metals. The errors range from −3 to 20% for Cr$K\alpha$ radiation and are almost as high for Ni. Over a limited range of sample types, the errors are more restricted, only 1.5–8.5% for granite and basalt.

Of course, SiO_2 is used here only as a reference and does not have to be used as a standard. The errors would be smaller if the standards and unknowns were of a similar rock type, but this would demand an unreasonably large number of standards. Hower's approximation could lead to serious errors if rocks of widely different types are analyzed. Carbonate rocks and iron titanium oxide ores may show especially large errors for some elements.

The results have an important implication in the preparation of standards. The preparation of standards by addition of trace elements to Al_2O_3, as suggested by Reynolds (1963), is likely to lead to large positive errors, except for analysis of bauxite and quartzite. This problem can be virtually eliminated by using the combined method, as presented below in Equations 19–31.

Table 2 shows that multiple uncompensated absorp-

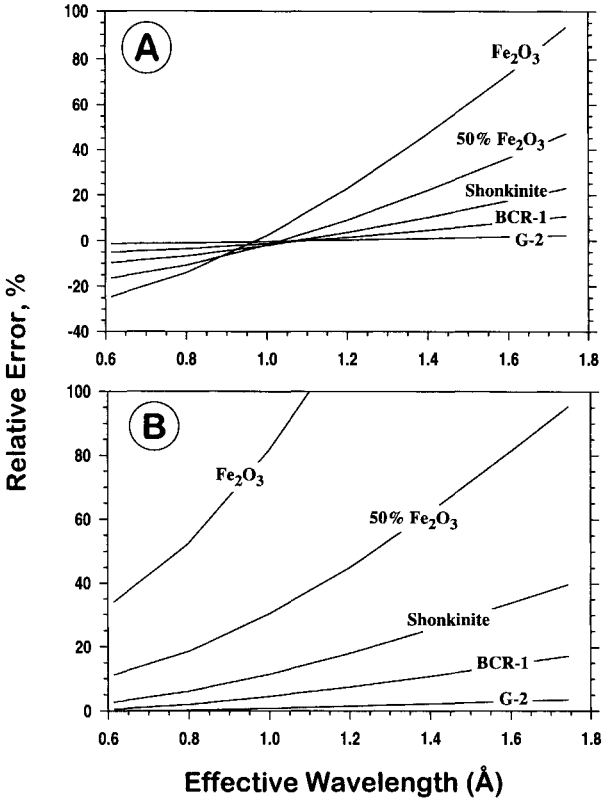

FIGURE 4. Errors in Cr concentrations calculated by the equivalent-wavelength method (Eq. 15), as a function of the assumed equivalent wavelength. Samples are G-2 (granite), BCR-1 (basalt), shonkinite (containing 34% SiO_2 and 35% Fe_2O_3), 50% Fe_2O_3–50% SiO_2, and Fe_2O_3 (see Table 1 for compositions). Rh tube, 44 kV, 22 target-takeoff angle, $\psi_1 = 55°$, $\psi_2 = 45°$, Be window thickness = 0.3 mm. Tube intensity from Pella et al. (1985), mass-absorption coefficients from Thinh and Leroux (1979). (**A**) Excluding errors due to enhancement. (**B**) Total errors, including errors due to uncompensated secondary fluorescence.

tion edges can cause significant errors. In granite G-2, Ni shows a 3% error. A pegmatitic granite, MA-N, which has 3600 parts per million (ppm) Rb and 173 ppm Nb, shows a 9% error for Ni. NIM-L is very unusual in having 960 ppm Nb, 4600 ppm Sr, and 1.1% Zr, which cause a 23% error in Ni.

COMPENSATION FOR ABSORPTION EDGES: THE EQUIVALENT-WAVELENGTH METHOD

Principles

A very simple method is often used to compensate for absorption edges without integrating over wavelength. According to the mean value theorem of calculus, there is at least one equivalent wavelength, $\lambda_e \leq \lambda_{edge\,i}$, such that Equation 1 can be rewritten as

$$I_{il} = C_i f_{il}(\lambda_{edge\,i} - \lambda_0)\frac{\mu_i(\lambda_e)I_0(\lambda_e)}{\mu'(\lambda_e) + \mu''(\lambda_i)}. \quad (15)$$

Secondary fluorescence is assumed to be insignificant. The expression $f_{il}(\lambda_{edge\,i} - \lambda_0)\mu_i(\lambda_e)I_0(\lambda_e)$ represents a calibration constant that is the same for all samples, and $\mu_s'(\lambda_e) + \mu_s''(\lambda_i)$ can be easily calculated from tables of mass-absorption coefficients. If Hower's approximation (Eq. 9) is valid, and if there is no significant (i.e., major element) absorption edge between the shortest incident wavelength and the analyte absorption edge ($\lambda_0 < \lambda < \lambda_{edge\,i}$), then λ_e is independent of the sample composition. Consequently, a single value of λ_e can be used for any such sample. The λ_e can be determined by numerical evaluation of Equation 1 and comparison with Equation 15. The equivalent wavelength must be determined once for each analyte element *i*, but it is not necessary to evaluate an integral for each sample.

Unfortunately, if there are intervening major element absorption edges, λ_e depends greatly on the sample composition because the shape of the integrand curve depends on the magnitude of the absorption-edge jump. Although Equation 15 is commonly used in such cases, it is not very accurate unless λ_e is evaluated individually for each element in each sample (a time-consuming and useless procedure!). An additional problem with Equation 15 is that it makes no correction for enhancement effects. Examples of errors owing to the use of Equation 15 are presented below.

Accuracy of the equivalent-wavelength method

The accuracy of the equivalent-wavelength method was determined by comparing the results of Equations 1 and 15, as described in the Appendix. An experimental test is also presented below in the section entitled "Experimental test of accuracy." The discontinuity caused by major element absorption edges means that the equivalent wavelength must be composition dependent, and that use of a single equivalent wavelength for all samples must cause calculation errors. Enhancement by secondary fluorescence may also be very significant.

Figure 4A shows errors in trace concentrations of Cr calculated using Equation 15, as a function of the assumed equivalent wavelength, considering only primary fluorescence. The results for granite G-2 suggest that the choice of equivalent wavelength is not critical for Fe-poor samples. The actual value is about 1.0 ± 0.1 Å. However, as expected, the equivalent wavelength is strongly dependent on the concentration of Fe, and for Fe-rich samples the analyst would have to select the correct wavelength for each sample.

However, Cr radiation is strongly enhanced in Fe-rich samples. It may not be possible to achieve acceptable accuracy without correcting for secondary fluorescence. Ignoring secondary fluorescence gives concentration errors of 11, 22, 46, and 86% for basalt BCR-1, shonkinite (see Table 2 for compositions), 50% Fe_2O_3–50% SiO_2, and Fe_2O_3, respectively.

The combined errors resulting from incorrect equivalent wavelength and neglected secondary fluorescence are shown in Figure 4B. For Fe ores there is no equivalent

wavelength, and calculation errors for Cr in Fe_2O_3 range from 34 to 243%. It appears that for analysis of Cr in these samples, the best choice of equivalent wavelength is the Rh$K\alpha$ wavelength at 0.62 Å rather than the actual value at about 1.0 Å. Thus, by compensating for one large error with another, it may be possible to obtain satisfactory results for samples with 35% FeO or less. Of course, it does not necessarily follow that this fortuitous compensation is valid for other analyte elements or for other analytical conditions.

Cr is certainly not the only element to be affected by strong enhancement effects. For example, secondary fluorescence by Fe causes concentration errors for Ba$L\alpha$ of 8, 18, 35, and 65%, respectively, for the four Fe-rich samples shown in Figure 4. Secondary fluorescence by 1.5% Zr causes a 5% error for Rb in NIM-L.

A NEW COMBINED COMPTON-PEAK-COEFFICIENT METHOD

Principles

Compton scattering of incident radiation can be used for approximate sample-matrix correction in the absence of absorption edges and enhancement effects, but it is necessary to solve Equation 1 directly or to use a coefficient method in other cases. It is possible to unify the Compton-peak and coefficient methods, to clarify the relation between them, and to combine their advantages: Coefficient methods make possible rapid, automatic corrections for virtually any sample composition, and the Compton-peak method is useful if the sample composition is not completely known.

The key is to formulate an exact expression for the sample mass-absorption coefficient as a function of wavelength, using Hower's approximation (Eq. 9) as the starting point. From Equation 5,

$$C_{Si}\mu_{Si}(\lambda) = \mu_S(\lambda) - \sum_{j\neq Si} C_j\mu_j(\lambda) \tag{16}$$

using Si as an arbitrary representative of typical wavelength dependence (see Fig. 3; SiO_2 can also be used). From Equations 9 and 16,

$$K(\lambda) = \frac{\mu_S(\lambda) - \sum_{j\neq Si} C_j\mu_j(\lambda)}{\mu_S(\lambda_t) - \sum_{j\neq Si} C_j\mu_j(\lambda_t)}. \tag{17}$$

It follows that

$$\mu_s(\lambda) = K(\lambda)\mu_s(\lambda_t) + \Sigma C_j[\mu_j(\lambda) - K(\lambda)\mu_j(\lambda_t)] \tag{18}$$

and

$$\mu_s^* = K^*\mu_s(\lambda_t) + \Sigma C_j[\mu_j^* - K^*\mu_j(\lambda_t)] \tag{19}$$

where

$$K^* = \frac{K(\lambda)}{\sin\psi_1} + \frac{K(\lambda_i)}{\sin\psi_2}. \tag{20}$$

Note that the expressions in brackets in Equations 18 and 19 are 0 for j = Si. Equations 18 and 19 express the sample mass-absorption coefficients in terms of known or determinable quantities, namely the composition and the sample mass-absorption coefficient at the tube wavelength. All other parameters can be calculated from published tables. The $\mu_s(\lambda_t)$ can be calculated from the composition or from the Compton-peak intensity, according to Equation 7.

Equations 18 and 19 open a whole new class of calculation methods. They can be used for direct solution of Equation 1 (the "fundamental parameters" method), or for calculation of influence coefficients, as follows. For a pure component, there is no secondary fluorescence, and the intensity I_{i0} for the pure component i is given by

$$I_{i0} = f_{il}\int A\frac{\mu_s^*}{\mu_i^*}\,d\lambda \tag{21}$$

where A and μ_s^* refer to the known or unknown multicomponent specimen (not the pure component), and μ_i^* refers to the pure component. If the intensity ratio (or apparent concentration) R_i is defined as I_{il}/I_{i0}, then

$$C_i/R_i = \frac{\int A\frac{\mu_s^*}{\mu_i^*}\,d\lambda}{\int A\,d\lambda + \sum C_j\int AE_j\,d\lambda} \tag{22}$$

and

$$C_i/R_i = \frac{\left(\frac{\int A\frac{\mu_s^*}{\mu_i^*}\,d\lambda}{\int A\,d\lambda}\right)}{1 + \sum C_j\left(\frac{\int AE_j\,d\lambda}{\int A\,d\lambda}\right)}. \tag{23}$$

Equation 19 is now substituted into Equation 23. The numerator is

$$\frac{\int A\frac{K^*\mu_S(\lambda_t)}{\mu_i^*}\,d\lambda + \int \sum C_jA\left[\frac{\mu_j^* - K^*\mu_j(\lambda_t)}{\mu_i^*}\right]d\lambda}{\int A\,d\lambda}. \tag{24}$$

The final result can be rewritten in coefficient form:

$$C_i/R_i = \frac{\mu_s(\lambda_t)\gamma_i + \sum_j C_j\beta_{ij}}{1 + \sum_j C_j\epsilon_{ij}} \tag{25}$$

where

$$\gamma_i = \frac{\int_{\lambda_0}^{\lambda_{edge\,i}} A\frac{K^*}{\mu_i^*}\,d\lambda}{\int_{\lambda_0}^{\lambda_{edge\,i}} A\,d\lambda} \tag{26}$$

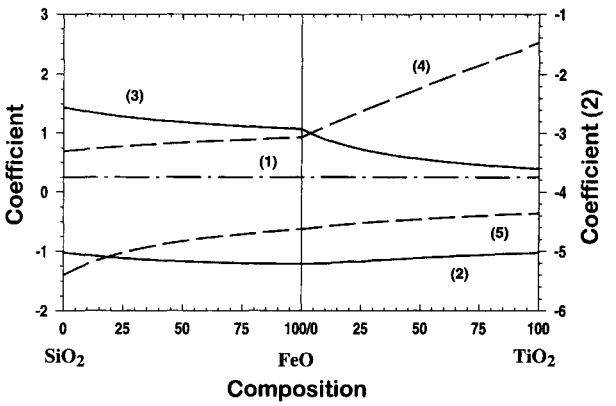

FIGURE 5. Variations of influence coefficients with composition, for analyte Cr, matrix element Fe, in the system SiO_2-FeO-TiO_2. Line 1 = γ_{Cr} for combined method (Eq. 26), 2 = $\beta_{Cr,Fe}$ for combined method (Eq. 27) (scale at right), 3 = enhancement coefficient ϵ_{ij} (Eq. 28), 4 = $1/\epsilon_{Cr,Fe}$, and 5 = $a_{Cr,Fe}$ for Lachance-Traill method (Eq. 32).

$$\beta_{ij} = \frac{\int_{\lambda_0}^{\lambda_{edge\,i}} A\left[\frac{\mu_j^*}{\mu_i^*} - \frac{K^*}{\mu_i^*}\mu_j(\lambda_i)\right] d\lambda}{\int_{\lambda_0}^{\lambda_{edge\,i}} A d\lambda} \quad (27)$$

and

$$\epsilon_{ij} = \frac{\int_{\lambda_0}^{\lambda_{edge\,i}} AE_j\, d\lambda}{\int_{\lambda_0}^{\lambda_{edge\,i}} A d\lambda}. \quad (28)$$

In Equation 25, γ_i and β_{ij} correct for sample absorption, and ϵ_{ij} corrects for enhancement effects. The $\mu_s(\lambda_t)$ can be calculated from the sample composition and mass-absorption coefficients, or from the Compton-peak intensity (Eq. 7).

Unfortunately, the coefficients depend on sample composition, as shown in Figure 5. Although γ_i and β_{ij} are relatively constant, ϵ_{ij} depends strongly on sample mass absorption. For many samples γ_i, β_{ij}, and ϵ_{ij} can be regarded as constants, but if there is strong secondary fluorescence, it is better to express the coefficients as functions of composition. One method is to expand the coefficients in series. Thus,

$$\gamma_i \approx \sum_k \gamma_{ik} C_k \quad (29)$$

and

$$\beta_{ij} \approx \sum_k \beta_{ijk} C_k \quad (30)$$

where γ_{ik} and β_{ijk} are the values of γ_i and β_{ij} in pure components k. This linear approach does not work well for ϵ_{ij}, but the expression

$$\frac{1}{\epsilon_{ij}} \approx \sum_k \frac{C_k}{\epsilon_{ijk}} \quad (31)$$

is much more accurate and is exact in some special cases. Although the basis is mainly empirical, it does give an excellent approximation, the accuracy of which is presented in the Discussion. Figure 5 presents an example of Cr enhancement by Fe, for which $1/\epsilon_{Cr,Fe}$ is nearly linear with composition. It must be emphasized that it is important for any coefficient method to be tested numerically over the entire range of expected sample compositions.

Other coefficient methods

Several coefficient methods, with varying degrees of validity, have been used (cf. Tertian and Claisse 1982; Pella et al. 1986). The best methods provide simple, automatic correction for absorption and enhancement, with accuracy that is very close to that provided by Equations 1, 25, and 29–31. Coefficient methods in general avoid the major errors of the Compton-peak and equivalent-wavelength methods.

The Lachance-Traill equation (cf. Rousseau 1984a; Tertian and Claisse 1982; Pella et al. 1986),

$$C_i/R_i = 1 + \sum_j C_j a_{ij} \quad (32)$$

is widely used for trace- and major-element analyses in diluted discs. Because the coefficients a_{ij} are known to depend largely on C_i (cf. Tertian and Claisse 1982, p. 160, 194; Pella et al. 1986), it is often assumed that a_{ij} depends only on C_i for trace elements and is therefore constant (because $C_i \approx 0$). Actually, if there is strong secondary fluorescence of the analyte element, the coefficients vary strongly with composition, as shown in Figure 5. Even so, it is possible to get acceptable results by assuming constant coefficients (R.M. Rousseau, personal communication; Pella et al. 1986). The values are customarily calculated for binary mixtures, each mixture consisting of the analyte component at its expected concentration and one matrix component ($C_i \approx 0$, $C_j \approx 1$ for trace elements). Ordinarily, oxide components are assumed (Pella et al. 1986). There are also many, more advanced algorithms that attempt to express the compositional dependence of the coefficients, while using as few coefficients as possible (cf. Tertian and Claisse 1982; Pella et al. 1986), although these are seldom used for trace element analysis.

Accuracy of coefficient methods

In this section the accuracy of coefficient methods is tested against the fundamental equation (Eq. 1), using the method described in the Appendix. Only the calculation errors in absorption-enhancement corrections are considered; experimental errors are additional. An experimental test is also described below in the section entitled "Experimental test of accuracy." The calculation errors are

TABLE 3. Accuracy of coefficient methods

Sample	Combined method*				Not expanded**	Lachance-Traill†
	Rb	Ni	Ba	Cr	Cr	Cr
Al_2O_3	−0.1	−0.0	−0.7	0.0	0.1	0.0
SiO_2	−0.2	−0.1	−0.6	−0.1	−0.0	−0.0
$FeSiO_3$	−0.2	−0.1	−1.4	−0.7	−4.0	4.8
Fe_2O_3	−0.1	−0.1	0.3	1.8	−0.9	1.5
$FeTiO_3$	−0.2	−0.1	−1.9	−1.0	−21.5	3.8
TiO_2	−0.2	−0.1	0.8	−0.2	−0.1	0.0
$CaFeSi_2O_6$	−0.2	−0.1	−1.3	−0.9	−10.0	3.7
$CaMg_{0.5}Fe_{0.5}Si_2O_6$	−0.2	−0.1	−0.9	−0.4	−5.7	2.3
SiO_2, 1% SrO	−0.2	0.0	−1.1	−0.0	0.0	−0.0
$ZrSiO_4$	5.1	1.1	−1.0	0.2	−21.9	0.8
ZrO_2	3.5	0.8	−1.0	0.2	−30.9	0.1
FeS_2	0.0	−0.0	−1.6	−1.8	−21.4	4.5
$CuFeS_2$	0.0	−0.2	−1.5	−1.8	−14.1	2.1
Shonkinite	−0.2	−0.1	−1.6	−1.0	−10.2	3.8
JF-2	−0.2	−0.1	−0.3	−0.0	−0.0	−0.0
G-2	−0.2	−0.1	−0.4	−0.2	−0.6	0.6
BCR-1	−0.2	−0.1	−0.8	−0.5	−3.1	2.3
NIM-L	−0.2	−0.0	−0.7	−0.5	−2.8	1.8
MA-N	−0.3	−0.0	−0.3	−0.1	−0.1	0.1

Note: Errors in weight percent.
* Combined method, expanded coefficients (Eqs. 25, 29–31).
** Combined method, constant (unexpanded) coefficients (Eq. 25).
† Lachance-Traill method, Equation 32.

shown in Table 3 for Rb, Ni, Ba, and Cr for several representative samples. It is not possible to prove the accuracy in all cases by example, but Table 3 shows several extreme cases that might be encountered for geologic materials. It is always advisable to test any method of approximation over the full range of effects to be encountered. The analyte elements represent a wide range of peak energies, and the samples include examples that show both strong absorption and strong enhancement of the analyte radiation. For a different perspective, results are also presented for several common rock types that show no such extreme effects.

The accuracy of the combined method (Eqs. 25 and 29–31) is excellent for all elements considered. We believe that it ranks among the best coefficient methods. Ti, Ca, and S strongly absorb Cr*K* and Ba*L* X-rays, and Fe produces strong secondary fluorescence. Yet the accuracy of Cr and Ba analysis is better than 2%, even in minerals that span an extreme compositional range. The accuracy for Ni is 0.2% or better in all samples, except in $ZrSiO_4$ and ZrO_2, where it is 1.1% or better. For the Lachance-Traill method, data are shown only for Cr, but the accuracy is about 5% or better for all elements considered.

Table 3 also shows results for Rb analysis in the SiO_2-ZrO_2 system because Zr causes very strong fluorescence of Rb. Even so, the combined method with expanded coefficients gives results that are accurate to about 5%.

Even without expanded coefficients (Eqs. 29–31) the results for Cr are fairly accurate in most samples. Even in Fe silicates and Fe_2O_3, the accuracy is 4% or better. However, $FeTiO_3$, FeS_2, and $CaFeSi_2O_6$ show strongly negative errors of more than 20% for Cr. The errors are indirectly due to the combination of strong secondary fluorescence and strong absorption by Ti, Ca, and S. Consequently, the use of expanded coefficients is generally recommended.

The accuracy of the combined method is also adequate for major element analysis in undiluted samples. Because of the effects of absorption edges, the concentration of Fe must be known for analysis of Ba, Co, Mn, Cr, and lighter elements, and the concentration of Ti must be known for Ba and Sc analysis. If a complete chemical analysis is not needed, it may be expedient or necessary to analyze pressed powder pellets for Fe and Ti. In any case, the required intensity data should be available because Fe and Ti intensities are required for spectral interference corrections. For the samples shown in Table 3 the accuracy of the combined coefficient method is 1.1% or better for Fe and 2.4% or better for Ti. This allows the analysis of trace elements from Sc ($Z = 21$) to U ($Z = 92$), plus Fe and Ti, on a single fused disk or pressed powder pellet.

Discussion of the combined method

Interpretation. The combined method amplifies and clarifies previous methods. The β_{ij} coefficients (Eq. 25) represent deviations from Hower's approximation (Eq. 9). Thus, for any matrix element j that conforms to Equation 9 over the appropriate wavelength interval, $\beta_{ij} = 0$. In addition, because $\beta_{ij} = 0$, element j has no absorption edge, so there is no enhancement, and $\epsilon_{ij} = 0$. If $\beta_{ij} = 0$ and $\epsilon_{ij} = 0$ for all j, then Equation 25 becomes

$$C_i/R_i = \mu_s(\lambda_t)\gamma_i. \tag{33}$$

Equation 33 represents the classical Compton method, in which $\mu_s(\lambda_t)$ is calculated from the Compton-peak intensity.

To the extent that $\beta_{ij} \neq 0$, the classical Compton-peak

TABLE 4. Influence coefficients for analyte Cr

Matrix element j	$\beta_{Cr,j}$	$\epsilon_{Cr,j}$
Li	−0.04	
B	−0.03	
C	−0.02	
O	0.00	
Na	−0.03	
Mg	0.03	
Al	0.03	
Si	0.00	
S	−0.10	
K	−0.38	
Ca	−0.55	
Ti	−0.69	
V	−3.54	
Mn	−4.46	0.15
Fe	−5.02	1.44
Zr	−16.05	0.81

Note: Rh tube, 44 kV; $\gamma_{Cr} = 0.25$.

method is inaccurate. Equation 25 provides a simple method for calculating the resulting errors. It is noteworthy that $\beta_{ii} \neq 0$, because the analyte element always has an absorption edge that affects the sample mass-absorption coefficient at the analyte wavelength. In a sense, any major element interferes with its own analysis, and it is not possible to analyze a major element by the unmodified Compton-peak method.

As an example, Table 4 shows the coefficients for Cr analysis. As noted previously, K and Ca deviate substantially from Equation 9 and therefore have nonzero $\beta_{Cr,j}$ coefficients. The value of $\beta_{Cr,Fe}$ is quite high because Fe has an absorption edge at 1.7 Å, which is well below the Cr$K\alpha$ wavelength of 2.1 Å. Fe and Mn have large ϵ_{ij} coefficients because they cause strong secondary fluorescence of Cr.

Partial chemical analysis. The combined method (Eq. 25) is especially useful for partial chemical analysis. Because the β_{ij} coefficients reflect only absorption edges or other deviations from Hower's approximation (Eq. 9), and are therefore generally small, it is not necessary to know the complete rock composition to correct for absorption and enhancement and to make an estimate of the errors resulting from incomplete information. As examples, for analysis of Cr in basalt and Ba in potassium feldspar, ignoring concentrations for elements with $Z <$ 20 (Ca) causes errors of 0.25 and 6.4%, respectively. Most other coefficient methods have generally larger influence coefficients and therefore require complete compositional information.

Partial chemical analysis is useful in many situations, especially if complete compositional information cannot be obtained or if limited information is required from each of many samples. One interesting application would be determination of concentration ratios for trace element–major element pairs. For example, Sr/Ca ratios could be determined in anorthosites and carbonates, Cr/Fe and V/Ti ratios in oxide ores, and Ba and Fe in Fe-rich hydrothermal deposits. Other applications include analysis of samples with major concentrations of second-row elements (Li through F), which cannot be easily analyzed by XRF. Finally, the method allows dilution of samples by materials that have incompletely known compositions (e.g., hydrocarbon binders), without any special matrix corrections for the binder.

In some cases it may be expedient or necessary to analyze for trace elements but not for major elements. The combined method makes this possible, even in samples with very high concentrations of Fe and Ti. Previous methods require a complete major element analysis for analysis for light transition elements (Sc, V, Cr, Co) and for Ba, Ce, and La (using L lines).

EXPERIMENTAL TEST OF ACCURACY

The overall accuracies of the combined method and the equivalent-wavelength method were evaluated experimentally for analysis of V in Fe-rich samples, as an example. V, like Cr, is subject to strong enhancement by Fe. In addition, the Fe absorption edge poses a problem for the Compton-peak and equivalent-wavelength methods. Thus, analysis of V in samples that contain highly variable concentrations of Fe constitutes a severe test of any XRF analytical method.

TABLE 5. Experimental analytical errors for analysis of V in Fe-rich samples, comparing three methods for absorption-enhancement corrections

Concentration		Error (% relative)*				
				Equivalent-wavelength method‡		
Fe_2O_3 (%)	V (ppm)	Fundamental Eqs.**	Combined method†	$\lambda_e = 0.62$ Å	$\lambda_e = 1.05$ Å	$\lambda_e = 1.7$ Å
0	*1770*	*−0.05*	*−0.05*	*−0.05*	*−0.05*	*−0.05*
0	*1706*	*0.05*	*0.05*	*0.05*	*0.05*	*0.05*
42	1469	0.33	−0.24	14.03	26.23	58.20
45	1981	−0.12	−0.68	14.37	27.57	62.18
89	2129	0.07	0.93	25.77	54.53	129.92
92	1592	−0.59	0.43	25.67	55.24	132.76

Note: Samples are $Fe_2O_3 + Al_2O_3 + V_2O_5$ mixtures fused with two parts of flux (75% $Li_2B_4O_7$, 25% $LiBO_3$). Rh tube, 55 kV, Siemens SRS-200.
* Al_2O_3 standards are shown in italics.
** Fundamental parameters method (Eq. 1), using Equation 19 for μ_s^*.
† Combined method, expanded coefficients (Eqs. 25, 29–31).
‡ Equivalent-wavelength method (Eq. 15), for different assumed equivalent wavelengths.

A series of samples was prepared by fusing mixtures of Al_2O_3, Fe_2O_3, and V_2O_5 with two parts of Li borate glass. Four samples containing up to 92% Fe_2O_3 were analyzed for V, using two Fe-free samples as standards. The results were evaluated using several of the equations presented above and are shown in Table 5.

The fundamental equations (1 and 19) give virtually perfect results, with <0.6% relative error for all samples. The new coefficient method (Eqs. 25 and 29–31), which represents a numerical approximation to the fundamental equations, gives results that are nearly as good, with relative errors of <1%. The results argue convincingly that the fundamental equations and the coefficient methods presented above are sound.

The equivalent-wavelength method (Eq. 15) gives relative errors between 14 and 133%, depending on the value assumed for the equivalent wavelength. As in the case of Cr, the errors are smaller if a very short wavelength is assumed for the equivalent wavelength, thereby offsetting some of the large errors resulting from secondary fluorescence with large negative errors.

Choice of methods

Influence-coefficient methods are clearly preferable to simple mass-absorption corrections (i.e., the equivalent-wavelength method or the unmodified Compton-peak method) because they allow automatic compensation for any number of absorption edges and complete correction for secondary fluorescence. It is also a great advantage that no special knowledge of the sample is required. A computer can do all needed calculations for any sample, with an exactly specified algorithm.

For routine trace element analysis, the Lachance-Traill method (Eq. 32) is a good choice if the sample composition is known completely. For greater accuracy, or if the sample composition is not known completely, the combined (new) method (Eqs. 25 and 29–31) can be used.

The combined method offers some special advantages and conveniences. As mentioned previously, it can be used for partial chemical analysis. Measurement of the Compton-peak intensity also compensates approximately for long-term variations in the tube intensity without requiring a monitor disc for each element that may be encountered. Because the Compton peak usually has a high count rate, the counting statistical errors may also be lower than if a monitor disc is used.

Acknowledgments

We thank Richard Rousseau, David Walker, John Hubbell, James Willis, Joe Taggart, Charles Wu, and Jacques Renault for reviews of the manuscript. We also thank James Willis for helping with trace element analysis and Richard Rousseau for the special thoroughness of his review. This work was partly funded by NSF grant EAR-9205351 for equipment.

References cited

Berger, M.J., and Hubbell, J.H. (1987) XCOM: Photon cross sections on a personal computer. U.S. Department of Commerce, NBSIR 87-3597.

Couture, R.A. (1993) Sample transparency effects in tin determination by X-ray fluorescence. X-ray Spectrometry, 22, 92–96.

Couture, R.A., Smith, M.S., and Dymek, R.F. (1993) X-ray fluorescence analysis of silicate rocks using fused glass discs and a side-window Rh source tube: Accuracy precision and reproducibility. Chemical Geology, 110, 315–328.

de Boer, D.K.G., Borstrok, J.J.M., Leenaers, A.J.G., van Sprang, H.A., and Brouwer, P.N. (1993) How accurate is the fundamental parameter approach? XRF analysis of bulk and multilayer samples. X-ray Spectrometry, 22, 33–38.

Eastell, J., and Willis, J.P. (1993) A low dilution fusion technique for the analysis of geological samples: 2. Major and minor element analysis and the use of influence/alpha coefficients. X-ray Spectrometry 22, 71–79.

Feather, C.E., and Willis, J.P. (1976) A simple method for background and matrix correction of spectral peaks in trace element determination by X-ray fluorescence spectrometry. X-ray Spectrometry 5, 41–48.

Govindaraju, K. (1989) 1989 compilation of working values and sample description for 272 geostandards. Geostandards Newsletter, 13, 1–113.

Harvey, P.K., and Atkin, B.P. (1982) The estimation of mass absorption coefficients by Compton scattering: Extensions to the use of Rh$K\alpha$ Compton radiation and intensity ratios. American Mineralogist, 67, 534–537.

Heinrich, K.F.J. (1986) Mass absorption coefficients for electron probe microanalysis. In J.D. Brown, Ed., Proceedings of the 11th International Congress on X-ray Optics and Microanalysis, p. 67–199. London, Ontario.

Hower, J. (1959) Matrix corrections in the X-ray spectrographic trace element analysis of rocks and minerals. American Mineralogist, 44, 19–32.

Hubbell, J.H., Veigele, W.J., Briggs, E.A., Brown, R.T., Cromer, D.T., and Howerton, R.J. (1975) Atomic form factors, incoherent scattering functions, and photon scattering cross sections. Journal of Physical Chemistry Reference Data, 4, 471–615.

Jenkins, R., Gould, R.W., and Gedcke, D. (1981) Quantitative X-ray spectrometry, 586 p. Dekker, New York.

Müller, R.O. (1972) Spectrochemical analysis by X-ray fluorescence, 326 p. Plenum, New York.

Pella, P.A., and Sieber, J.R. (1982) Intercomparison of selected semi-empirical and fundamental parameter interelement correction methods in X-ray spectrometry. X-ray Spectrometry, 11, 167–169.

Pella, P.A., Liangyuan, F., and Small, J.A. (1985) An analytical algorithm for calculation of spectral distributions of X-ray tubes for quantitative X-ray fluorescence analysis. X-ray Spectrometry, 14, 125–135.

Pella, P.A., Tao, G.Y., and Lachance, G. (1986) Intercomparison of fundamental parameter interelement correction methods, Part 2. X-ray Spectrometry, 15, 251–258.

Reynolds, R.C., Jr. (1963) Matrix corrections in trace element analysis by X-ray fluorescence: Estimation of the mass absorption coefficient by Compton scattering. American Mineralogist, 48, 1133–1143.

——— (1967) Estimation of mass absorption coefficients by Compton scattering: Improvements and extensions of the method. American Mineralogist, 52, 1493-1502.

Rousseau, R.M. (1984a) Fundamental algorithm between concentration and intensity in XRF analysis: I. Theory. X-ray Spectrometry 13, 115–120.

——— (1984b) Fundamental algorithm between concentration and intensity in XRF analysis. II. Practical application. X-ray Spectrometry 13, 121–125.

Rousseau, R.M., and Bouchard, M. (1986) Fundamental algorithm between concentration and intensity in XRF analysis: III. Experimental verification. X-ray Spectrometry, 15, 207–215.

Sherman, J. (1955) The theoretical derivation of fluorescent X-ray intensities from mixtures. Spectrochimica Acta 7, 283–306.

Shiraiwa, T., and Fujino, N. (1966) Theoretical calculation of fluorescent X-ray intensities in fluorescent X-ray spectrochemical analysis. Japanese Journal of Applied Physics, 5, 886–899.

Sparks, C.J. (1975) Quantitative X-ray fluorescence analysis using fundamental parameters. Advances in X-ray Analysis, 19, 19–51.

Tertian, R., and Claisse, F. (1982) Principles of quantitative X-ray fluorescence analysis, 385 p. Heyden, London, U.K.

Thinh, T.P., and Leroux, J. (1979) New basic empirical expression for computing tables of X-ray mass attenuation coefficients. X-ray Spectrometry, 8, 85–91 [erratum, X-ray Spectrometry, 10, p. v (1981)].

Walker, D. (1973) Behavior of X-ray mass absorption coefficients near absorption edges: Reynolds' method revisited. American Mineralogist, 58, 1069–1072.

Manuscript received March 10, 1995
Manuscript accepted January 31, 1996

Appendix: Calculation of errors in the Compton-peak and equivalent-wavelength methods

The combined errors resulting from Hower's approximation (Eq. 9) and from multiple trace element absorption edges were calculated by dividing the results of Equation 11, which gives the approximate value, by the results of Equation 1, which gives the exact value. (The secondary fluorescence term in Eq. 1 was ignored for the purpose of these comparisons.) By recalculating and renormalizing compositions to exclude elements with intervening absorption edges, the same procedure was used to calculate the error resulting from Hower's approximation alone. The difference is due to multiple trace element absorption edges.

It is important to remember that the same calculation errors apply to both the unknown sample and a standard, so that the net concentration error depends on both the sample and the standard. For these estimates the standard was assumed to be SiO_2 with a trace of the analyte. The following mathematical method was used for the estimates. The Compton-peak intensity can be calculated directly (Hubbell et al. 1975), or it can be calculated to an excellent degree of approximation from Equation 7. SiO_2 and λ_t were used as references to calculate $K(\lambda)$. From Equations 1, 7, and 11, the concentration ratio is given by

$$\frac{C_{calc}}{C_{actual}} = \frac{I_{il,sample}}{I_{il,SiO_2}} \frac{\mu_s(\lambda_t)}{\mu_{SiO_2}(\lambda_t)} \quad \text{(A-1)}$$

where values of I_{il} for the sample and SiO_2 are calculated from Equation 1 (again ignoring secondary fluorescence).

The errors due to the equivalent-wavelength method can be calculated in a very similar way. The error is given by

$$\frac{C_{calc}}{C_{actual}} = \frac{I_{il,sample}}{I_{il,SiO_2}} \left[\frac{\mu'_{SiO_2}(\lambda_e) + \mu''_{SiO_2}(\lambda_i)}{\mu'_s(\lambda_e) + \mu''_s(\lambda_i)} \right]. \quad \text{(A-2)}$$

The error due to neglecting secondary fluorescence is

$$\frac{C_{calc}}{C_{actual}} = \frac{\int A\,d\lambda + \sum_j C_j \int AE_j\,d\lambda}{\int A\,d\lambda}. \quad \text{(A-3)}$$